Inverse design of incoherent Raman pump sources for U-band WDM transmission over 125 km G.652.D fiber

Tangyanjun Lan[1], Junjiang Xiang[1], Gai Zhou[1,2,3,*], Meng Xiang[1,2,3], Songnian Fu[1,2,3], *Senior Member, IEEE*, and Yuwen Qin[1,2,3,*]

[1]Institute of Advanced Photonics Technology, School of Information Engineering, Guangdong University of Technology, Guangzhou 510006, China

[2]Key Laboratory of Photonic Technology for Integrated Sensing and Communication, Ministry of Education of China, Guangdong University of Technology, Guangzhou, 510006, China

[3]Guangdong Provincial Key Laboratory of Information Photonics Technology, Guangdong University of Technology, Guangzhou, 510006, China

***Abstract*—The ever-increasing demand for the transmission capacity has stimulated intensive investigations, in terms of both new transmission window of standard single mode fiber (SSMF) and new fiber utilizing the spatial domain. Multi-band wavelength division multiplexing (WDM) transmission exploring the extended wavelength band, besides traditional C+L band, is an attractive solution for the rapid and cost-effective enhancement of transmission capacity. To this end, here we demonstrate the U-band WDM transmission over 125-km G.652.D fiber, when the C-band amplified spontaneous emission (ASE) source acts as the incoherent pump for Raman amplification (RA). Meanwhile, bidirectional long short-term memory neural network (BiLSTM-NN) is applied to inversely design the spectral shape of two C-band ASE sources. After the optimization through inverse design, the ROP variation at the U-band can be less than 1.2 dB under different net Raman gains. Consequently, we can experimentally achieve a net Raman gain of ~15 dB over a 3 dB bandwidth of around 2.1 THz at the U-band, under the condition of distributed bidirectional Raman pump configuration. Finally, the performance of the U-band RA is experimentally verified by transmitting three-wavelength 20 GBaud DP-QPSK signals, when the threshold of 7% HD-FEC can be successfully reached.**

***Index Terms*—Raman amplifier, neural network, inverse design, WDM transmission.**

I. INTRODUCTION

With the continuous advancement of various network applications, the demand of transmission capacity is constantly increasing [1]. The enhancement of transmission capacity can be achieved through two schemes. One is to use a new type of space division multiplexing fiber, while the other is to explore new transmission windows of traditional standard single mode fiber (SSMF). Currently, extending the new transmission window and achieving wavelength-division multiplexing (WDM) transmission are ideally desired. With regard to the deployed SSMF, the C-band (1530~1565 nm) has been comprehensively utilized, as it holds the lowest transmission loss window, together with the invention of erbium-doped fiber amplifier (EDFA) to compensate the corresponding transmission loss [2]. However, the C-band potential has been effectively explored by the dense WDM(DWDM) technique. Recently, in order to solve the challenge of SSMF capacity crunch, both S-band (1460~1530 nm) and L-band (1565~1625 nm) have gained the attention of telecom carriers, because the optical amplifier can be developed to mitigate the transmission loss in each band [3]. Although both O-band (1260~1360 nm) and E-band (1360~1460 nm) transmission loss values arising in the SSMF are a little bit higher than that of U-band (1625~1675 nm), both are ready for the short-reach photonic interconnection [4]. Therefore, current long-haul WDM transmission is mainly concentrated at the C- and L-band [5, 6], but few demonstrations related to the U-band has been reported. One of the main challenges is the availability of high-performance optical amplifier [4]. In fact, there occur several specifically doped fiber amplifiers that are suitable for the U-band transmission, including bismuth-doped fiber amplifier (BDFA), praseodymium-doped fiber amplifier (PDFA) and thulium-doped fiber amplifier (TDFA). Although those doped fiber amplifiers can provide optical gain at U-band, they all have their own disadvantages. BDFA has low power conversion efficiency at the U-band [7], and some optical amplification characteristics of bismuth are still not well understood [8, 9]. The utilization of PDFA is hampered by the need of a fluoride-glass substrate and high pump power [8]. TDFA typically requires the use of high-power pump and the amplified spontaneous emission (ASE) inhibition at longer wavelengths [10, 11]. In addition to the above-mentioned fiber optics amplifiers, semiconductor optical amplifiers (SOAs) can also be designed to provide the U-band gain. However, the used materials of the U-band SOAs need further optimization, and its amplification performance suffers from poor noise figure (NF), higher polarization sensitivity, and stronger inter-channel crosstalk [12].

Apart from the EDFA and SOA, Raman amplifier (RA) is also a viable option for providing the U-band gain, as it can offer low noise properties due to the distributed amplification and theoretically provide gain at arbitrary wavelength in case

(*Corresponding author: gaizer3085@gdut.edu.cn, qinyw@gdut.edu.cn).

the suitable pump source is available [13]. Since the central wavelength of U-band is 1650 nm, the corresponding wavelength of Raman pump is located at ~1550 nm, which is exactly at the C-band. There are abundant laser sources and high-power optical amplifiers available, and the pump light can be transmitted over the SSMF with minimal loss. Since the U-band Raman gain efficiency is reduced, in comparison with the C- and L-Band, the availability of high-power pumps is very important for U-band RA [8]. Most importantly, Raman amplifiers are flexible to shape its gain profile by properly adjusting the pump power spectrum. This is a critical characteristic of next-generation multi-band WDM transmission, as individual channel power profile that maximizes the corresponding transmission bit rate is not the same, due to both Kerr nonlinearity and stimulated Raman scattering [14, 15].

An early experimental demonstration of U-band RA based on the backward pump configuration can provide a peak gain of 31.6 dB, a gain bandwidth of more than 50 nm, a gain fluctuation of less than 1.5 dB, and a NF of less than 6.5 dB [16]. Such presentation explores the gain characteristics of RA suitable for the U-band. Recently, incoherent pump source has been experimentally proposed for the realization of U-band RA over 40-km non-zero dispersion shifted fiber (NZDSF), achieving a net gain of 21.7 dB and a NF of ~4 dB over the wavelength range from 1646.7 nm to 1669.9 nm [4]. The use of incoherent pump source has several merits, including both the reduction of relative intensity noise [17] and the achievement of gain flattening profile [18]. In particular, the U-band RA can be conveniently realized by the use of C-band ASE source, such as EDFA, as a broadband incoherent pump source. Moreover, the detailed characterization of the bidirectional ASE pump configuration is helpful to realize the 9.2 GBaud DP-BPSK transmission over 285 km NZDSF. However, the impact of ASE spectral shape on the Raman gain characteristic and the potential of U-band WDM transmission are still unknown.

The design of the RA gain profile in early days was mainly through solving a series of nonlinear differential equations describing the propagation of pumps and signals along the fiber[19]. However, no solution has been proven to be applicable to the design of arbitrary Raman gain profile so far [20]. In recent years, with the development of neural networks (NNs), attempts have been made to use NNs in the inverse design of C-band RA to obtain a desired gain profile, under the condition of the CW pumps [20]. In this paper, we propose using NN to inversely design the spectral shape of broadband incoherent pump source, in order to equalize the received optical power (ROP) variation among several U-band wavelengths. Compared with other studies, we use broadband incoherent pump source under the bidirectional pump configuration, with the gain region at U-band, and focus on the inverse design of the spectral shape of the incoherent pump source. We choose bidirectional long short-term memory neural network (BiLSTM-NN), because it holds expressive power without increasing the amount of data required, leading to the risk reduction of underfitting in comparison with other NN structures [21]. Simulation results show that the ROP variations of the standard ASE pump are 1.58 dB, 2.26 dB and 3.26 dB, respectively, under 0 dB, 10 dB and 20 dB net gains, for the

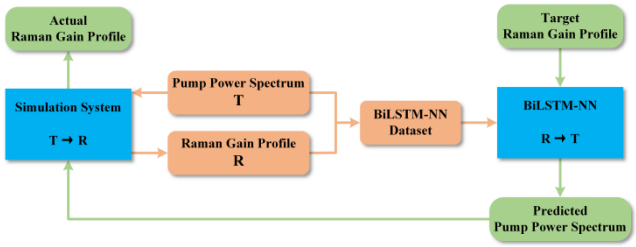

Fig. 1. Schematic diagram of inverse design based on neural network. **R** denotes the Raman gain profile set and **T** denotes the pump power spectrum set.

standard. In contrast, the ROP variation by the inverse design incoherent pump is always less than 1.2 dB. Based on the inverse-design spectral shapes, we experimentally demonstrate the U-band 20 GBaud DP-QPSK signals WDM transmission over 125-km G.652.D fiber, where two optimized ASE sources are utilized to realize a bidirectional RA.

The rest of the paper is organized as follows. In Section II, we introduce a BiLSTM-NN-based inverse design strategy to identify the optimal spectral profile of C-band ASE sources, where the objective is to equalize the ROP variation among U-band WDM channels. In Section III, we present the experimental WDM transmission results and corresponding discussions between the theoretical results and the experimental conditions. Section IV summarizes all conclusions of current submission.

II. BILSTM-NN-BASED INVERSE DESIGN

In this section, we use BiLSTM-NN to inversely design the spectral shape of broadband incoherent pump, in order to obtain the desired Raman gain profile and achieve the least ROP variation over the wavelength range of 1645-1660 nm. Fig. 1 shows the schematic diagram of inverse design. The dataset for NN training and validation includes pump power spectrum **T** and Raman gain profile **R**, which are generated by the numerical simulation. The complex mapping relationship between **T** and **R** is learned by a BiLSTM-NN. After completing the training and validation of the NN, we utilize the target Raman gain profile as the input of NN to predict the optimal spectral shape of incoherent pump source. In addition, the predicted spectral shape of incoherent pump source will be imported into the simulation system again, for the ease to obtain

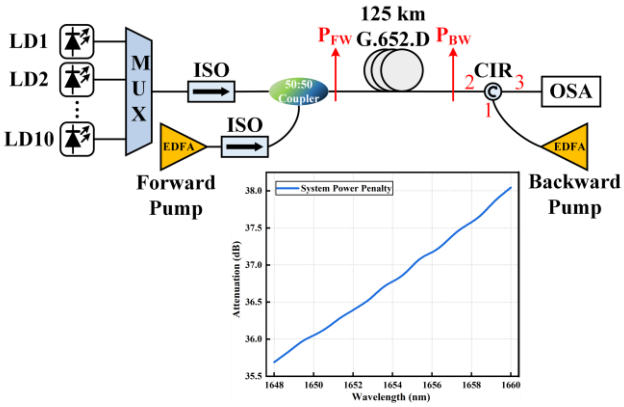

Fig. 2. Simulation schematic diagram. The inset is the system power penalty from 1645 nm to 1660 nm.

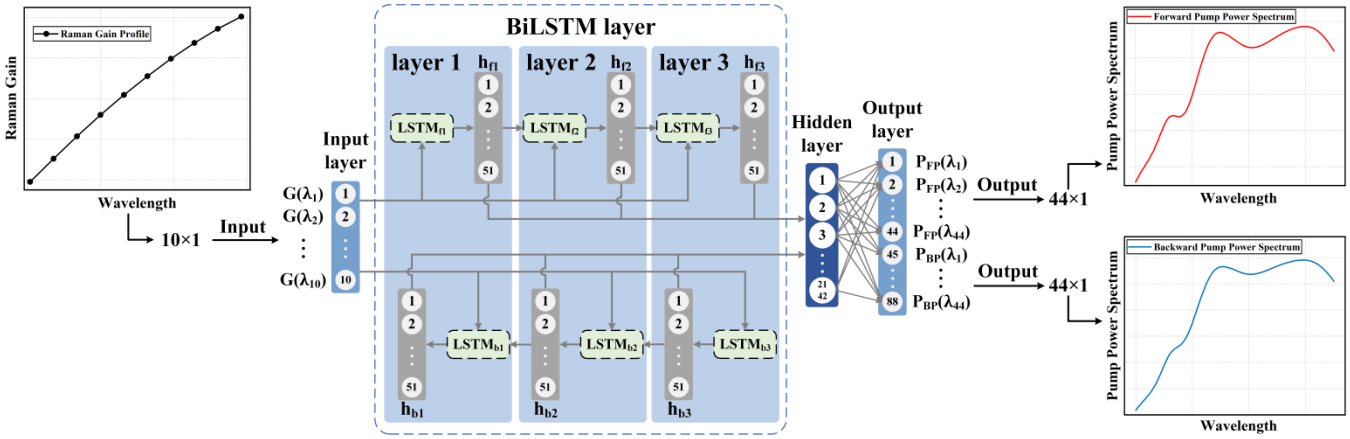

Fig. 3. Architecture of BiLSTM-NN for broadband incoherent pump shape inversely designed with an input, BiLSTM, hidden and output layers.

the Raman gain profile, and compare it with the target Raman gain profile, in order to evaluate whether the predicted spectral shape can satisfy the design requirements.

As shown in Fig. 2, the simulation system is built up with the commercial VPI software. We use a total of 10 U-band lasers with different wavelengths, each with a launch power of -25 dBm. The wavelength range of all lasers is from 1645 to 1660 nm, with an interval of 1.6 nm. To further explore the influence of pump power on the inverse design of Raman gain profile, we obtain NN datasets with 0 dB, 10 dB and 20 dB net gains through simulation, and use those three datasets for the BiLSTM-NN training and validation. The wavelength referenced for the net Raman gain change is 1652 nm, located at the center of the selected wavelength range in the U-band. The forward pump powers P_{FW} corresponding to 0 dB, 10 dB and 20 dB net gains are 28 dBm, 29 dBm and 30 dBm, respectively, and the backward pump powers P_{BW} are 29 dBm, 30 dBm and 31 dBm. The SSMF length is 125 km, while its transmission loss from 1645 nm to 1660 nm is characterized by the use of a supercontinuum light source in the experiment. After including the 6 dB loss of 50:50 optical coupler and CIR, the power penalty from 1645 nm to 1660 nm is indicated in the inset of Fig. 2. In order to obtain sufficient data for training and validating the NN, we consider various pump spectral shapes, including rectangle, Gaussian distribution, positive slope tilts, negative slope tilts, convex triangles, concave triangles, and random distributions. Among them, both rectangular and Gaussian distributions only contain one situation. The power standard deviation of Gaussian distribution is 20 mW. Both tilted shapes contain 7 situations, ranging from a difference of 1 dB between the maximum and minimum pump powers at each wavelength to a difference of 7 dB between the maximum and minimum values. Both triangles contain 7 different situations, similar to the tilted shape, ranging from a difference of 1 dB between the maximum and minimum pump powers at each wavelength to a difference of 7 dB between the maximum and minimum values. The random distributions include 10 situations, ranging from random fluctuations of pump power within 1 mW at each wavelength to random fluctuations within 5 mW, with two sets of data for each fluctuation situation. Fig. 4 shows several typical pump shapes. In Fig. 4, except for rectangular and Gaussian distribution shapes, the showcase of other pump shapes corresponds to the situation of maximum fluctuation. In summary, we have considered a total of 40 different pump shapes. Due to the bidirectional pump configuration used in the system, both the forward and backward pumps contain 40 different pump shapes. By pairing the different shapes of the forward and backward pumps, we obtained 1600 sets of data at each net Raman gain. Each dataset contains the Raman gain profile and its corresponding forward and backward pump power spectra, which are used as the input data and output labels of BiLSTM-NN.

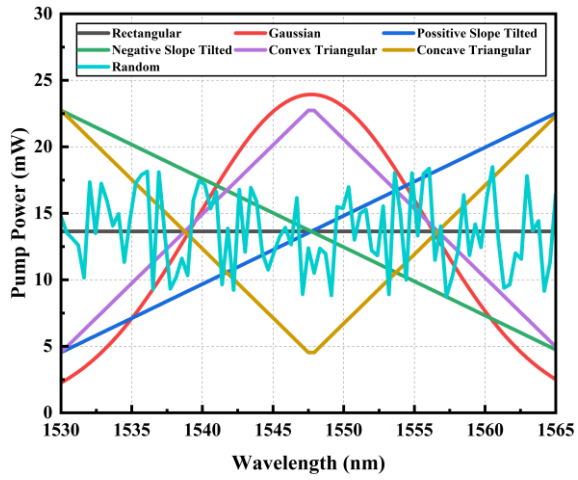

Fig. 4. Several typical pump shapes.

The architecture of the three-layer BiLSTM-NN for the inverse design of incoherent pump source is illustrated in Fig. 3. In each LSTM layer, both the forward and backward LSTM contain 51 neurons, and all of the generated state vectors of each layer are merged into the hidden layer of the NN. The BiLSTM-NN-based optimization is driven by the input Raman gain profiles and output pump power spectrum. The learning rate of BiLSTM-NN is 0.0005, and the activation functions of the BiLSTM-NN are tanh function and sigmoid function. In order to better process the training data and labels, we have performed sampling operations on the power spectrum of broadband incoherent pump source, simplifying the data operation while ensuring the fitting of the spectral shape. We sample the power spectrum of forward and backward incoherent pump sources at the C-band, with 44 sampling points for each pump, and an interval of 100 GHz between each point. By using the Raman

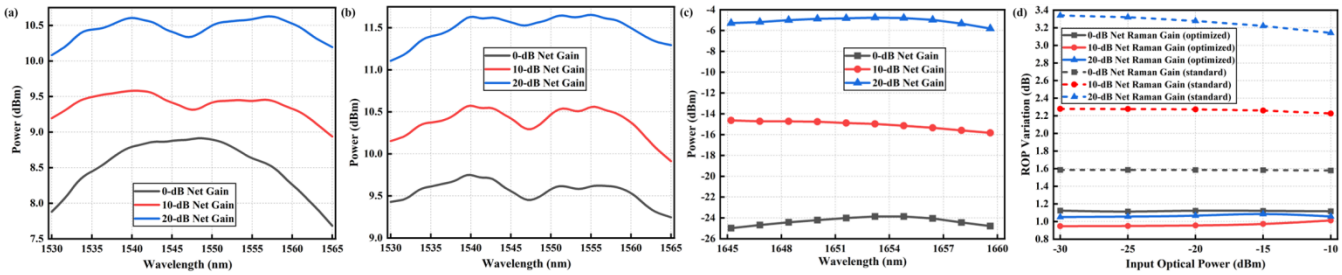

Fig. 5. (a) Forward incoherent pump power spectrum shape corresponding to 0, 10, 20 dB net Raman gains. (b) Backward incoherent pump power spectrum shape corresponding to 0, 10, 20 dB net Raman gains. (c) ROPs at different wavelengths under 0, 10, 20 dB net gains. The shape of the incoherent pump power spectrum used is obtained through the inverse design. (d) The ROP variation versus input optical power. Two cases of optimized pump (obtained through inverse design) and standard pump are under consideration.

gain of 10 channels at the U-band as the input data, and the 88 power spectrum samples as the corresponding labels for the NN, we obtain the dataset required for NN training and validation.

After the training and validation of BiLSTM-NN, we input the target gain profile into the well-trained BiLSTM-NN to obtain the spectral shape of broadband incoherent pump sources. It should be noted that, the wavelength dependences of the RA gain and system power penalty need to cancel out. As shown in Fig. 5 (a) and (b), a dip at 1647 nm is observed for the inversely designed spectra of both incoherent pump sources. With the growing net gain, the dip of forward pump deepens while that of the backward pump flattens. We import the pump power spectrum output by BiLSTM-NN into the VPI software, in order to obtain the corresponding gain profile. The ROP variation versus the wavelength is shown in Fig. 5 (c). The ROP variation is 1.12 dB, 1.20 dB and 1.06 dB, respectively, in the case of 0 dB, 10 dB, and 20 dB minimum net gain. In Fig. 5 (d), we compare the ROP variation between the use of the BiLSTM-NN-based inverse design pump and the standard ASE pump, when the input power is varied from -30 dBm to -10 dBm. The spectral shape of the standard ASE pump is obtained by measuring the commercial EDFAs in our lab. There occurs a significant difference, in term of ROP variation of 1.58 dB, 2.26 dB and 3.26 dB, respectively, under 0 dB, 10 dB and 20 dB net gains, for the standard ASE pump. In contrast, the ROP variation by the inverse design incoherent pump is always less than 1.2 dB under three different net gains. Above results indicates that, the proposed inverse design strategy for the incoherent pumped RA can effectively equalize the ROP variation of the U-band WDM signals.

III. U-BAND WDM TRANSMISSION

In this section, according to the inverse design results, we select the EDFA with the highest similarity in spectral shape in our laboratory as the incoherent pump sources, and realize the U-band WDM transmission over the 125-km G.652.D fiber.

The experimental setup of U-band WDM transmission is shown in Fig. 6. 20 GBaud DP-QPSK signals are modulated on three optical carriers with wavelengths of 1648 nm, 1654 nm and 1660 nm, by the use of a C-band coherent driver modulator (CDM) with 3-dB bandwidth of 35 GHz. Before coupling with the forward incoherent pump, the signal power of each channel is ~-26 dBm. In the distributed RA, the powers of forward and backward incoherent pumps are P_{FW} = 26.5 dBm (~447 mW) and P_{BW} = 30.2 dBm (~1.05 W), respectively. After transmission, the ROP of WDM signal is adjusted by a VOA and the signal is detected by a C-band integrated coherent receiver (ICR) with 3-dB bandwidth of 40 GHz. Since the channel spacing of the WDM signal is 6 nm, there is basically no channel crosstalk so that we do not use corresponding optical bandpass filter, which is unavailable in our laboratory. The wavelength channel under test is selected by switching the laser source injected to the local oscillation (LO) of the ICR. The electrical signal from the ICR is collected by a real-time oscilloscope with 80 GSa/s sample rate. Finally, the digital signal processing is implemented and its transmission performance is evaluated by the bit error ratio (BER).

Fig. 7 (a) presents the spectrum of the output signal. The powers of three channels at 1648 nm, 1654 nm and 1660 nm are -10.86 dBm, -9.93 dBm and -8.39 dBm, respectively, leading to a ROP variation of ~2.47 dB among three wavelength

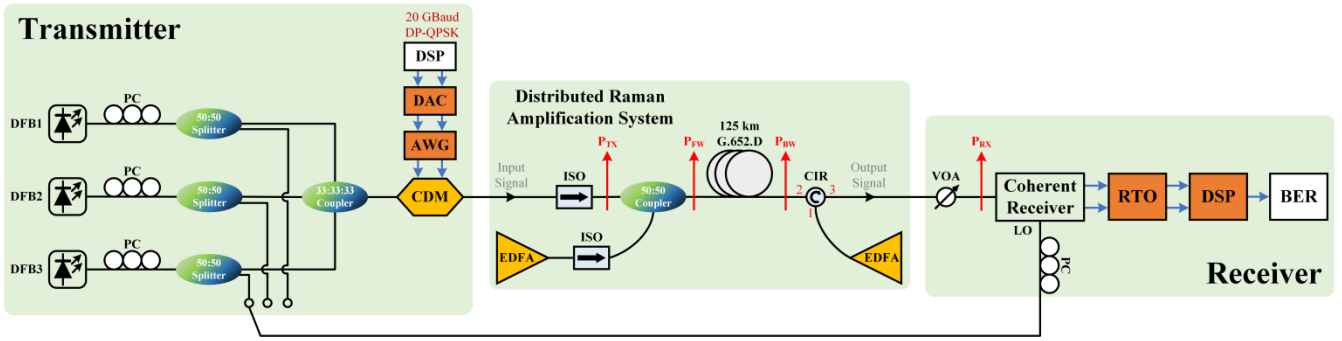

Fig. 6. Experimental setup of U-band WDM transmission based on broadband incoherent pump sources under the bidirectional Raman pump configuration.

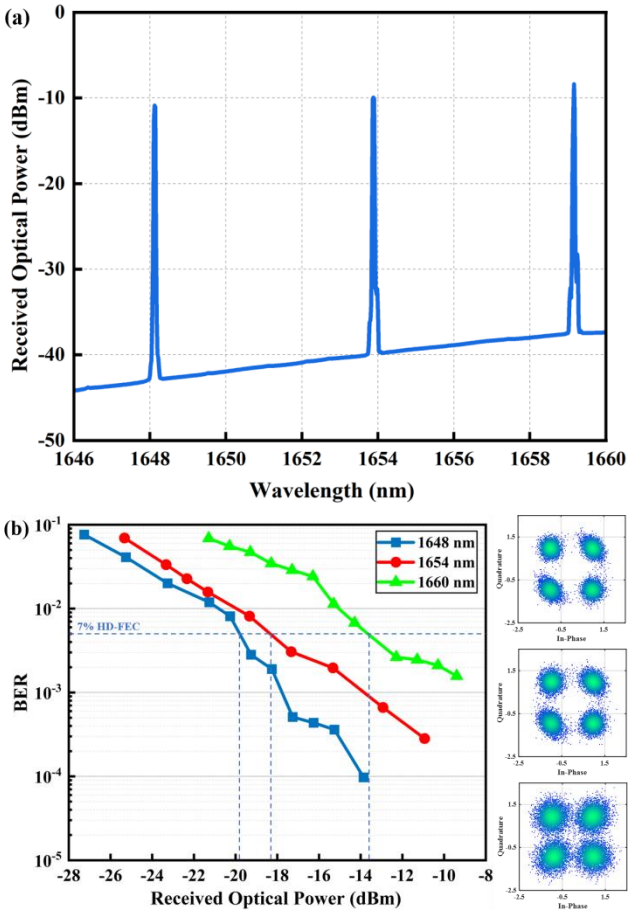

Fig. 7. (a) Received spectrum of the U-band WDM signal. (b) BER versus ROP after transmission. The insets are the X-polarization constellations of each channel at ROP = -16 dBm.

channels. We believe that a better result can be anticipated in case the spectral shape of incoherent pump source is obtained according to the inverse design results. As shown in Fig. 7 (b), we study the BER of each wavelength channel versus the ROP, and present the X-polarization constellations of each channel with ROP = -16 dBm. The BER performance increase with the channel wavelength under the same ROP. This is because the responsivity of the C-band ICR degrades rapidly at U-band. In this experiment, the ROP values of three channels at 1648 nm, 1654 nm and 1660 nm to reach the 7% hard decision forward error correction (HD-FEC) threshold are around -19.5 dBm, -17.8 dBm and -13.8 dBm, respectively. In summary, a 224 Gb/s U-band WDM transmission over 125-km G.652.D fiber can be achieved, with the help of incoherent pump-based RA.

IV. CONCLUSIONS

In this paper, we propose to design the distributed RA gain profile by inversely designing the spectral shape of incoherent pump sources based on BiLSTM-NN, in order to equalize the ROP variation of U-band WDM signals. Simulation results show that the ROP variation can be less than 1.2 dB in the case of 0 dB, 10 dB, and 20 dB minimum net gain with the inversely designing the pump source. Based on the inversely designed results, we successfully demonstrate U-band three-wavelength 20 GBaud DP-QPSK signals transmission over 125 km G.652.D fiber, under the condition of bidirectional Raman pump configuration. We believe that those results will encourage further investigation of the U-band long-haul SSMF transmission.

ACKNOWLEDGEMENT

This work was supported in part by National Natural Science Foundation of China (U21A20506, 62205068), Guangdong Introducing Innovative and Entrepreneurial Teams of “The Pearl River Talent Recruitment Program” (2021ZT09X044).

REFERENCES

[1] Cisco, *Cisco Visual Networking Index Forecast and Trends, 2017–2022 White Paper*. May. 2019.

[2] E. Agrell *et al.*, "Roadmap of optical communications," *Journal of Optics*, vol. 18, no. 6, p. 063002, 2016.

[3] R. Sadeghi *et al.*, "Transparent vs Translucent Multi-Band Optical Networking: Capacity and Energy Analyses," *Journal of Lightwave Technology*, vol. 40, no. 11, pp. 3486-3498, 2022, doi: 10.1109/JLT.2022.3167908.

[4] N. Taengnoi, K. R. H. Bottrill, Y. Hong, L. Hanzo, and P. Petropoulos, "Ultra-Long-Span U-band Transmission Enabled by Incoherently Pumped Raman Amplification," *Journal of Lightwave Technology*, pp. 1-7, 2023, doi: 10.1109/JLT.2023.3265172.

[5] S. Escobar-Landero, X. Zhao, A. Lorences-Riesgo, D. L. Gac, Y. Frignac, and G. Charlet, "Modeling and Optimization of Experimental S+C+L WDM Coherent Transmission System," in *2023 Optical Fiber Communications Conference and Exhibition (OFC)*, 5-9 March 2023, pp. 1-3, doi: 10.1364/OFC.2023.Th3F.4.

[6] F. Hamaoka, M. Nakamura, M. Takahashi, T. Kobayashi, Y. Miyamoto, and Y. Kisaka, "173.7-Tb/s Triple-Band WDM Transmission using 124-Channel 144-GBaud Signals with SE of 9.33 b/s/Hz," in *2023 Optical Fiber Communications Conference and Exhibition (OFC)*, 5-9 March 2023, pp. 1-3, doi: 10.1364/OFC.2023.Th3F.2.

[7] S. V. Firstov *et al.*, "A 23-dB bismuth-doped optical fiber amplifier for a 1700-nm band," *Scientific Reports*, vol. 6, no. 1, pp. 28939, 2016/06/30, doi: 10.1038/srep28939.

[8] L. Rapp and M. Eiselt, "Optical Amplifiers for Multi–Band Optical Transmission Systems," *Journal of Lightwave Technology*, vol. 40, no. 6, pp. 1579-1589, 2022, doi: 10.1109/JLT.2021.3120944.

[9] E. M. Dianov, "Bismuth-doped optical fibers: a challenging active medium for near-IR lasers and optical amplifiers," *Light: Science & Applications*, vol. 1, no. 5, pp. e12-e12, 2012/05/01, doi: 10.1038/lsa.2012.12.

[10] S. Chen *et al.*, "Ultra-short Wavelength Operation of a Thulium Doped Fiber Laser in the 1620–1660nm Wavelength Band," in *2018 Optical Fiber Communications Conference and Exposition (OFC)*, 11-15 March 2018, pp. 1-3.

[11] C. Jiang, "Proposal of a Pr^{3+}-doped telluride fiber amplifier for 1.3, 1.49, and 1.6 μm transmission windows," *Appl. Opt.*, vol. 47, no. 36, pp. 6811-6815, 2008/12/20, doi: 10.1364/AO.47.006811.

[12] P. P. Baveja, D. N. Maywar, A. M. Kaplan, and G. P. Agrawal, "Self-Phase Modulation in Semiconductor Optical Amplifiers: Impact of Amplified Spontaneous Emission," *IEEE Journal of Quantum Electronics*, vol. 46, no. 9, pp. 1396-1403, 2010, doi: 10.1109/JQE.2010.2048743.

[13] R. Stolen and E. Ippen, "Raman gain in glass optical waveguides," *Applied Physics Letters*, vol. 22, no. 6, pp. 276-278, 1973.

[14] F. Hamaoka *et al.*, "Ultra-Wideband WDM Transmission in S-, C-, and L-Bands Using Signal Power Optimization Scheme," *Journal of Lightwave Technology*, vol. 37, no. 8, pp. 1764-1771, 2019, doi: 10.1109/JLT.2019.2894827.

[15] A. Ferrari *et al.*, "Multi-Band Optical Systems to Enable Ultra-High Speed Transmissions," in *2019 Conference on Lasers and Electro-Optics Europe & European Quantum Electronics Conference (CLEO/Europe-EQEC)*, 23-27 June 2019, pp. 1-1, doi: 10.1109/CLEOE-EQEC.2019.8872247.

[16] P. C. Reeves-Hall, D. A. Chestnut, C. J. S. De Matos, and J. R. Taylor, "Dual Wavelength Pumped L and U-Band Raman Amplifier," in *Optical Amplifiers and Their Applications*, Stresa, 2001/07/01: Optica Publishing Group, in OSA Technical Digest Series, p. OMC4, doi: 10.1364/OAA.2001.OMC4. [Online].

[17] M. A. Iqbal, M. Tan, and P. Harper, "RIN Transfer Mitigation Technique Using Broadband Incoherent Pump in Distributed Raman Amplified Transmission Systems," in *2018 20th International Conference on Transparent Optical Networks (ICTON)*, 1-5 July 2018, pp. 1-4, doi: 10.1109/ICTON.2018.8473635.

[18] Z. Ting, Z. Xiupu, and Z. Guodong, "Distributed fiber Raman amplifiers with incoherent pumping," *IEEE Photonics Technology Letters*, vol. 17, no. 6, pp. 1175-1177, 2005, doi: 10.1109/LPT.2005.846479.

[19] B. Neto, A. J. Teixeira, N. Wada, and P. André, "Efficient use of hybrid genetic algorithms in the gain optimization of distributed Raman amplifiers," *Opt. Express*, vol. 15, no. 26, pp. 17520-17528, 2007.

[20] D. Zibar, A. M. R. Brusin, U. C. d. Moura, F. D. Ros, V. Curri, and A. Carena, "Inverse System Design Using Machine Learning: The Raman Amplifier Case," *Journal of Lightwave Technology*, vol. 38, no. 4, pp. 736-753, 2020, doi: 10.1109/JLT.2019.2952179.

[21] X. Li and X. Zheng, "A Study of the BiLSTM Model Based on WOA Optimized Attention Mechanism for Power Load Forecasting," in *2023 IEEE International Conference on Sensors, Electronics and Computer Engineering (ICSECE)*, 18-20 Aug. 2023, pp. 237-242, doi: 10.1109/ICSECE58870.2023.10263362.